HAL
open science

Contribution to the study of fission products release from nuclear fuels in severe accident conditions: effect of the pO 2 on Cs, Mo and Ba speciation

Claire Le Gall, F. Audubert, Jacques Léchelle, Yves Pontillon, Jean-Louis F Hazemann

To cite this version:

Claire Le Gall, F. Audubert, Jacques Léchelle, Yves Pontillon, Jean-Louis F Hazemann. Contribution to the study of fission products release from nuclear fuels in severe accident conditions: effect of the pO 2 on Cs, Mo and Ba speciation. EPJ N - Nuclear Sciences & Technologies, 2020, 6, pp.2. 10.1051/epjn/2019058 . cea-02458380

HAL Id: cea-02458380

https://cea.hal.science/cea-02458380v1

Submitted on 28 Jan 2020

HAL is a multi-disciplinary open access archive for the deposit and dissemination of scientific research documents, whether they are published or not. The documents may come from teaching and research institutions in France or abroad, or from public or private research centers.

L'archive ouverte pluridisciplinaire **HAL**, est destinée au dépôt et à la diffusion de documents scientifiques de niveau recherche, publiés ou non, émanant des établissements d'enseignement et de recherche français ou étrangers, des laboratoires publics ou privés.

EPJ Nuclear Sci. Technol. **6**, 2 (2020)
© C. Le Gall et al., published by EDP Sciences, 2020
https://doi.org/10.1051/epjn/2019058

EPJ Nuclear Sciences & Technologies

Available online at:
https://www.epj-n.org

Regular Article

Open Access

Contribution to the study of fission products release from nuclear fuels in severe accident conditions: effect of the pO_2 on Cs, Mo and Ba speciation

Claire Le Gall[1,*], Fabienne Audubert[1], Jacques Léchelle[1], Yves Pontillon[1], and Jean-Louis Hazemann[2]

[1] CEA, DEN / DEC, Cadarache, 13108 Saint-Paul-Lez-Durance, France
[2] Institut Néel, CNRS – UGA & CRG – FAME, ESRF, 38041 Grenoble cedex 9, France

Received: 30 October 2019 / Accepted: 15 November 2019

Abstract. The objective of this work is to experimentally investigate the effect of the oxygen potential on the fuel and FP chemical behaviour in conditions representative of a severe accident. More specifically, the speciation of Cs, Mo and Ba is investigated. These three highly reactive FP are among the most abundant elements produced through ^{235}U and ^{239}Pu thermal fission and may have a significant impact on human health and environmental contamination in case of a light water reactor severe accident. This work has set out to contribute to the following three fields: providing experimental data on Pressurized Water Reactor (PWR) MOX fuel behaviour submitted to severe accident conditions and related FP speciation; going further in the understanding of FP speciation mechanisms at different stages of a severe accident; developing a method to study volatile FP behaviour, involving the investigation of SIMFuel samples manufactured at low temperature through SPS. In this paper, a focus is made on the impact of the oxygen potential towards the interaction between irradiated MOX fuels and the cladding, the interaction between Mo and Ba under oxidizing conditions and the assessment of the oxygen potential during sintering.

1 Introduction

At the time of rising concerns about greenhouse gases emission and confronted to an increase of the world needs in energy, nuclear power appears as a sustainable solution that intends to develop across the world. Guaranteeing the safety and security of the existing and future nuclear facilities is thus a top priority. Nowadays, 65% of the nuclear reactors in the world are PWR. These very complex facilities are composed of fuel pellets (UO_2 or MOX $(U,Pu)O_2$) piled up in a Zirconium (Zr) alloy cladding tubes placed in a vessel containing water at around 350 °C under 150 bars. These pellets are thus submitted to important strains (temperature, pressure, radiation, etc.) linked to both the fission reaction of heavy nuclei they contained and to the reactor's design.

Despite the constant improvements made on the safety systems implemented in the reactors, failures might happen and lead, in very rare cases, to nuclear severe accidents. These events, implying melting of all or part of the nuclear core, might also lead to radioactive materials release in the environment, as demonstrated in the cases of Chernobyl (1986) and Fukushima-Daiichi (2011). In addition, the damaged core remains hardly accessible even years after the accident because of the radiations it is still emitting. Among the numerous elements that are potentially released during such an accident, some fission products have a strong radiological impact. Moreover, their volatility can vary due to their high chemical reactivity and the physical-chemical evolution of the fuel. It is notably the case of Cesium (Cs), Molybdenum (Mo) and Barium (Ba).

Quantify the source term, corresponding to the nature and quantity of radioactive materials released during a severe accident, is thus a critical issue to:
– precisely estimate the consequences on populations and the environment,
– take decisions in term of crisis management,
– understand the chronology of the accident and predict the final state of the reactor's core,
– securely dismantle the facility in the long term.

To do so, models are developed and validated thanks to the results of experimental programs aiming at reproducing and understanding some phenomena occurring during a

* e-mail: legall.claire1@gmail.com

This is an Open Access article distributed under the terms of the Creative Commons Attribution License (https://creativecommons.org/licenses/by/4.0), which permits unrestricted use, distribution, and reproduction in any medium, provided the original work is properly cited.

severe accident. However, the remaining uncertainties concerning the behaviour of the different systems involving the fuel, the cladding, Cs, Mo and Ba in severe accident conditions limit the current source term prediction capacities of these models.

In this framework, the objective of this work was to experimentally investigate the effect of the oxygen partial pressure (pO_2) and temperature on the fuel and fission products chemical behaviour in conditions representative of a severe accident. Two types of samples have been studies in detail: irradiated MOX fuels and simulated high burn-up UO_2 fuels produced through sintering at high temperature (1650 °C, 2 h, H_2 atmosphere). The samples were submitted to thermal treatments in conditions representative of a PWR severe accident. This approach made it possible to cover a large temperature range from 400 °C up to 2530 °C and oxygen potentials from $-470\,\mathrm{kJ\,mol_{(O2)}}^{-1}$ to $-100\,\mathrm{kJ\,mol_{(O2)}}^{-1}$.

Experimental data were interpreted thanks to thermodynamic calculations performed using ThermoCalc [1] coupled with the TAF-ID database [2], currently developed by OECD. They were then confronted to existing data on Cs, Mo and Ba speciation used in source term prediction models.

The high temperature sintering process used to produce SIMFuels prevents Cs confinement within the UO_2 matrix. Thus, a Spark Plasma Sintering (SPS) route was developed in collaboration with the Joint Research Centre of Karlsruhe. This process enabled obtaining dense samples containing Cs, Mo and Ba at 1200 °C under Ar in 5 min. Thermodynamic calculations were performed using Factsage coupled with the SGPS database [3,4] in order to better explain the different phenomena occurring during SPS.

2 Experimental methods

As explained in the introduction and detailed in the following section, three different types of samples were studied in this work to investigate the impact of the oxygen partial pressure on the fuel and FP behaviour during a severe accident:

- Three irradiated MOX fuels enabled to study the impact of the cladding on the fuel's microstructure evolution under both oxidizing and reducing atmosphere at very high temperatures. The effect of the fuel-cladding interaction on FP behaviour has also been assessed.
- SIMFuel samples sintered at high temperature made it possible to probe Mo and Ba speciation in conditions representative of intermediate stages of a severe accident, notably thanks to XAS experiments unavailable, up to now, on irradiated fuels.
- SIMFuel samples sintered through SPS were developed to study Cs speciation under severe accident conditions as Cs cannot be confined in SIMFuels sintered at high temperature. The contribution of thermodynamics to this work axis was particularly important to assess the pO_2 conditions in the sintering furnace.

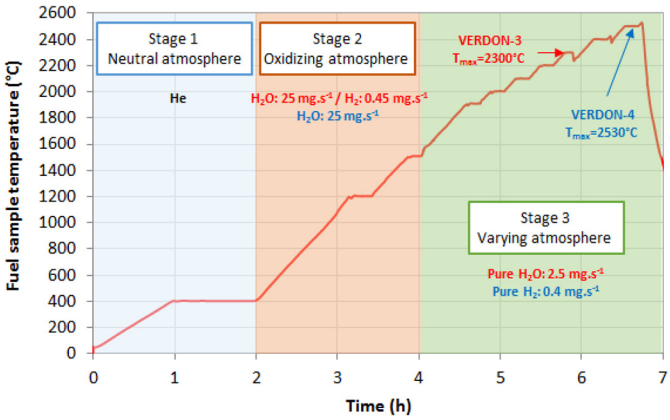

Fig. 1. Thermal sequence of the VERDON-3 and 4 tests.

2.1 Irradiated fuels

2.1.1 Samples description

The three samples studied in this part were extracted from the FXP2CC-B05 father rod which consisted in MOX-E fuel irradiated 4 cycles in a PWR operated by EDF. The local burn-up of the segment where the three samples were taken from was around 60 GWd t_{HM}^{-1}.

One of the three irradiated samples was characterized as irradiated and is termed $T_{0(IF)}$ in the following sections whereas the two other samples underwent the VERDON-3 and VERDON-4 tests described hereafter. Before the VERDON experiments, the samples were re-irradiated at low linear power ($\approx$20 W cm^{-1}) in the OSIRIS Material Testing Reactor for nine days to recreate the short half-life FP without any in-pile release.

2.1.2 VERDON tests

The samples were placed vertically in a hafnia crucible in the VERDON furnace, described in detail in [5,6]. The main objective of the VERDON-3 and 4 complementary tests was the study of MOX fuel behaviour and FP release under oxidizing (VERDON-3) and reducing (VERDON-4) conditions at very high temperature (>2300 °C). The different stages of the VERDON-3 and 4 tests are summarized in Figure 1.

The atmosphere during the test was imposed by the equilibrium of H_2O/H_2. Thermodynamic calculations were performed using the Thermo-Calc [1] software coupled with the TAF-ID database [2] in the conditions of stages 2 and 3 of the VERDON-3 and 4 tests. The evolution of the oxygen potential during stages 2 and 3 has been calculated from the H_2O/H_2 system by integration of the whole quantity of gas injected during the step considered (Fig. 2).

2.1.3 Characterizations

Detailed characterizations were performed on the $T_{0(IF)}$ sample and the samples retrieved after the VERDON-3 and 4 tests. The objective was to study the evolution of the different phases observed in the fuel. OM and SEM observations enabled to study the microstructure of the

Table 1. Final composition of the SIMFuel samples (the difference to 100% is due to the O content) and description of the additives used to synthesize the SIMFuel samples.

Elements	U	Ba	Ce	La	Mo	Sr	Y	Zr	Rh	Pd	Ru	Nd
Content (at%)	29.60	0.19	0.32	0.18	0.59	0.13	0.06	0.58	0.06	0.32	0.59	0.64
Additives	UO_2	$BaCO_3$	CeO_2	La_2O_3	MoO_3	SrO	Y_2O_3	ZrO_2	Rh_2O_3	PdO	RuO_2	Nd_2O_3

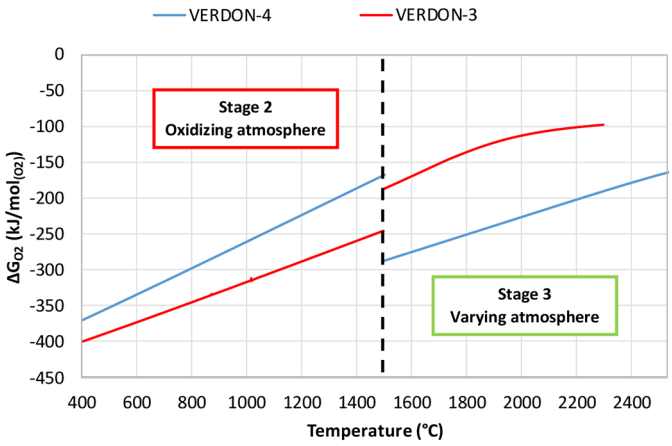

Fig. 2. Evolution of the oxygen potential during the stage 2 and 3 of the VERDON-3 and 4 tests, calculated from the H_2O/H_2 system using Thermo-Calc [1] coupled with the TAF-ID [2].

samples. SIMS isotope mapping and X-ray maps enabled to determine FP location and associations in the fuel samples. Mass spectra were also recorded on different regions of the samples mainly to discriminate Zr coming from the cladding and Zr produced by fission within the fuel. EPMA quantitative profiles helped quantifying the amount of the different elements present in the fuel samples. These characterizations were performed in different locations along the radius of the pellets, 0R being the centre and 1R the periphery.

Thermodynamic calculations were performed using the Thermo-Calc [1] software coupled with the TAF-ID database [2] in the conditions of stages 2 and 3 of the VERDON-3 and 4 tests. The objective was to help interpreting the experimental data and to assess the TAF-ID performances in the case of calculations on irradiated fuels. No calculations were performed on the first stage of the VERDON tests because the sample is not at thermodynamic equilibrium.

2.2 SIMFuel samples sintered at high temperature

2.2.1 Samples description

The samples were synthesized with depleted UO_2 from batch TU2-792 (Areva NC) produced through wet route. The initial average stoichiometry of the powder was 2.20 (mixture of mainly $UO_{2.01}$ and U_4O_9). Eleven additives were used to simulate the major FP created in irradiated fuels except volatile FP. They were mainly added under oxide form or a carbonate form in the case of Ba (Tab. 1). The initial quantities of FP surrogates were weighted to correspond to the composition of a PWR UO_2 fuel with a burn-up of 76 GWd $t_{HM}{}^{-1}$, calculated using the CESAR code [7].

Sample preparation was carried out in a glovebox according to the procedure described in [8,9]. The eleven FP surrogates were mixed together and added to UO_2. Planetary milling with Al_2O_3 balls was performed during 30 min in ethanol to achieve a well homogeneous dispersion of the additives in the matrix. The resulting slurry was dried in an oven and sieved first at 1000 µm and then at 160 µm. Pre-compaction (50 MPa), pressing (450 MPa) and sintering at 1650 °C for 2 h under flowing H_2 were then performed.

2.2.2 Thermal treatment conditions

Thermal treatments were performed in the DURANCE experimental loop located in the UO_2 laboratory described in [6,10]. A polished disk of SIMFuel is placed in a metallic W crucible within an induction furnace. The pO_2 in the inlet gas (Ar + 4% H_2) is controlled in input of the loop thanks to a zirconia oxygen pump. The pO_2 is also measured in input and output of the loop thanks to two MicroPoas probes (provided by Setnag) maintained at 650 °C (Gen'air and Jok'air respectively). The temperature below the crucible is monitored by a thermocouple during the tests.

Two campaigns of tests were carried. They consisted in a temperature ramp of 20 °C s^{-1} followed by a dwell time of 2 h at 400 °C, 700 °C, 900 °C, 1000 °C and 1700 °C under controlled pO_2. The pO_2 was maintained at 1.97×10^{-20} atm ($H_2O/H_2 = 50$) at 650 °C in the case of the "oxidizing" campaign and at 5.08×10^{-27} atm ($H_2O/H_2 = 0.02$) in the case of the "reducing" campaign. The gas flow was set at 40 mL min^{-1}.

Only the results of the "oxidizing" campaign will be treated in this paper. As shown in Table 2, the evolution of the oxygen potential during these tests is in the same range compared to the ones of the stage 2 of the VERDON-3 and 4 tests.

2.2.3 Characterizations

Detailed characterizations were performed on the SIMFuels as-sintered ($T_{0(SIMF)}$) and after the different thermal treatments to study the chemical evolution of the different phases observed in these samples. These characterizations included density measurements, OM and SEM observations

Table 2. Experimental conditions used to perform the "oxidizing" thermal treatments.

Sample's name	O400	O700	O900	O1000
Temperature during the test (°C)	400	700	900	1000
Oxygen potential (kJ mol^{-1})	–387.73	–340.30	–308.22	–292.05

that enabled describing the evolution of the microstructure after the different treatments. X-ray maps and local EDX analyses were performed on the whole range of elements present in the SIMFuel samples but only the ones expected to compose the different phases of interest are shown (Mo, Ru, Rh, Pd, O and U in the case of metallic precipitates and Ba, Zr, Sr, Y, Ce, O and U in the case of the oxide precipitates). These analyses coupled to XANES measurements were performed in order to study the chemical evolution of the phases observed in the samples. More specifically, XANES measurements allowed to study Mo and Ba speciation in the different samples. XANES calculations using the FDMNES software [11] were performed when some reference samples were missing, in order to interpret the experimental spectra.

Only the results obtained on the $T_{0(SIMF)}$ and O1000 samples will be presented in the rest of this paper.

2.3 SIMFuel sintered through SPS

2.3.1 Fabrication process

Eight batches of SIMFuels were sintered (one was made out of pure UO_2) with different combinations of additives (Cs uranates, Cs or Ba molybdates, $BaCO_3$ or MoO_3). In this paper, only two batches of samples will be detailed: batch 3 ($UO_2 + 1.2$ wt%$Cs_2U_xO_y$) and 8 ($UO_2 + 4$ wt%$Cs_2U_xO_y + 4$ wt% $BaMoO_4$). The compositions of batch 3 is representative of a PWR UO_2 fuel with a burn-up of 76 GWd $t_{HM}{}^{-1}$, calculated using the CESAR code [7]. Batch 8 was synthesized with higher concentrations in FP surrogates to enable easier the characterizations.

Commercial depleted UO_2 (Cogema) was first pre-reduced at 800 °C during 4h under Ar + 6.5% H_2 in order to avoid a stoichiometry gradient in the pellets after sintering and to limit the deviation from stoichiometry of the as-sintered pellets [12]. Commercial MoO_3, $BaMoO_4$, Cs_2MoO_4 and $BaCO_3$ were used as received. Cesium uranate was synthesized according to the protocol described in [13]. The composition of the final orange powder was characterized through XRD to be a mixture between Cs_2UO_4 (22%), $Cs_2U_2O_7$ (75%) and Cs_2O (3%). For the sake of clarity, in the following chapter, the Cs uranates will be termed as $Cs_2U_xO_y$.

Sample preparation was carried out in a glovebox under Ar atmosphere. The additives powders were first ground separately in an agate mortar. The pre-reduced UO_2 was then added to the mixture which was ground again manually. The powder was finally poured into a 6 mm diameter SPS matrix made out of graphite and containing a graphite foil to ease the extraction of the pellet after sintering. Graphite disks were also placed between the pistons and the powder to prevent the pellet from being stuck to the pistons. A pre-compaction step was performed at 500 N (~17.7 MPa) and the following cycle was run: the gas was evacuated from the sintering chamber and a pressure of ~88 MPa was applied to the powder. The chamber was then filled with Ar and heated up to the final temperature (1200 °C, 200 °C/min) maintained during 5 min. Finally, the furnace was cooled down and the pressure was released.

2.3.2 Characterizations

The characterizations performed on the SIMFuels sintered through SPS included density measurements and SEM observations that enabled studying the microstructure of the samples, notably the grain size and FP distribution in the pellets. EDX analyses and XANES experiments were also carried out on these samples in order to determine FP chemical state and more especially Cs speciation. Finally, quantitative chemical analyses using ICP-AES and ICP-MS [14] were used to quantify FP release after sintering.

Predominance diagrams were established using the Phase Diagram module of the FactSage 7.0 software coupled to the SGPS database [3,4]. Only temperature and oxygen potential were set as variables. The elemental concentrations were determined using the results of chemical analyses performed on the samples, when available. Some redox indicators have been added to the diagrams:

- the equilibrium $C_{(s)}/CO_{(g)}$ at 0.1 and 1 bar,
- the equilibrium $CO_{(g)}/CO_{2(g)}$ at 1 bar,
- the oxygen potential corresponding to stoichiometric UO_2 in the calculation range of temperature,
- the oxygen potential corresponding to $UO_{2.01}$ in the calculation range of temperature.

3 Main results and discussion

3.1 Irradiated fuel's microstructure evolution

The post-test examination of the VERDON-3 and 4 samples highlighted a change of microstructure after both tests linked notably to an interaction between the fuel and the cladding. This can clearly be observed in the micrographs of the three samples in Figure 3. The fuel-cladding interaction zone progressed from 5 µm in the $T_{0(IF)}$ sample's periphery up to 200 µm in the VERDON-3 sample without melting. This is not surprising as liquid would have stated to be formed in the VERDON-3 conditions above the maximal temperature of the texts (2300 °C), at 2420 °C, according to thermodynamic

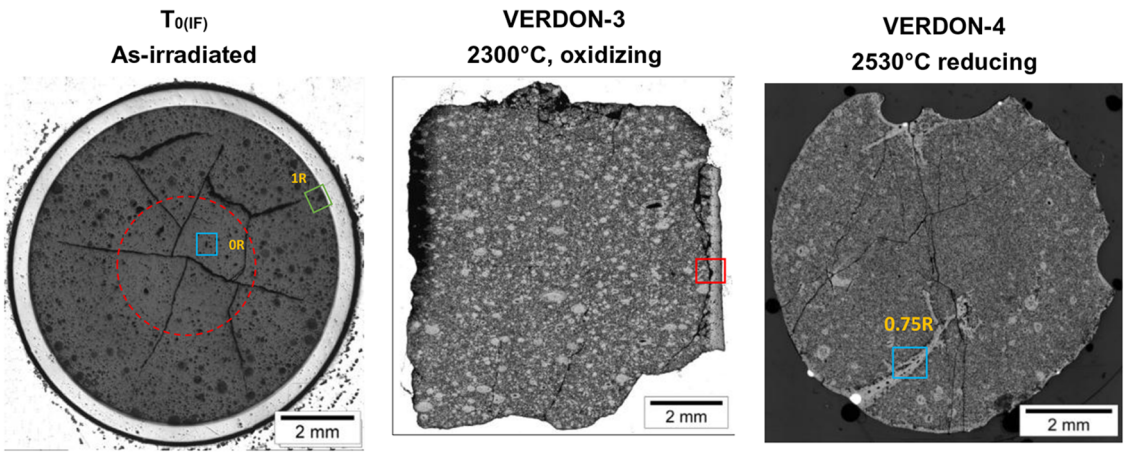

Fig. 3. Micrographs of the three irradiated samples under study.

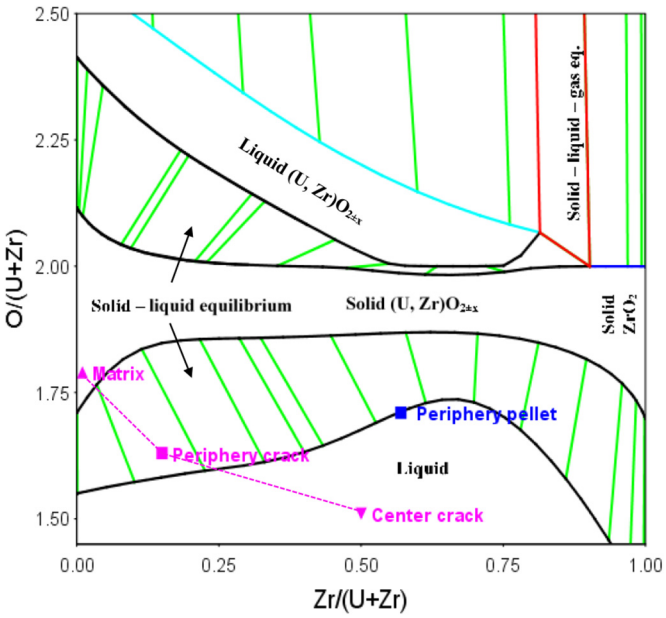

Fig. 4. Calculated isotherm diagram of the Zr/(U+Zr) content as a function of O/(U+Zr) at 2530 °C where the experimental data obtained in the molten regions at the periphery of the sample and in the the crack found at 0.75R of the VERDON-4 samples are reported, calculated with Thermo-Calc [1] and the TAF-ID [2].

calculations. However, this interaction led to the melting and progression of a $U_yZr_{1-y}O_{2\pm x}$ phase through the cracks of the fuel sample during the VERDON-4 test.

The final compositions of the liquid phase were measured experimentally in the periphery of the VERDON-4 sample, and crossing the crack found at 0.75 R from the UO_2 matrix until the centre of the crack. They have been reported on the isotherm diagram presented in Figure 4 and calculated using the ThermoCalc coupled with the TAF-ID [1,2]. As indicated in this diagram, the compositions measured in these points are consistent with the tie lines orientation. Moreover, a Zr enrichment is observed in the periphery of the pellet (1R) compared to the centre of the crack at 0.75R. This confirms the hypothesis made in [15], assuming progressive dissolution of UO_2 coming from the fuel matrix by the liquid $U_yZr_{1-y}O_{2\pm x}$ phase originally formed at the periphery when temperature increased:

- First, Zr-U interdiffusion occurs until a certain $U_yZr_{1-y}O_{2\pm x}$ composition is reached.
- Melting of this $U_yZr_{1-y}O_{2\pm x}$ phase occurs as soon as the composition meeting the minimum melting temperature is reached (probably around 2480 °C in the test conditions according to thermodynamics calculations).
- The molten phase then penetrates through the cracks of the pellet leading to progressive dissolution of the fuel by $U_yZr_{1-y}O_{2\pm x}$.
- The melt is then reduced as the temperature increases.

Metallic precipitates also known as white inclusions have been observed across the three samples under study. They are common in irradiated fuels [16]. In the VERDON-3 and 4 samples, these precipitates differed by their size and location. Indeed, their size varied from around 1 µm up to 200 µm. The larger precipitates were only found in the molten zones at the periphery of the VERDON-4 sample whereas in the rest of the sample, smaller precipitates were mainly located in the Pu agglomerates, as it was the case in $T_{0(IF)}$.

Given the rounded flatten shape of these precipitates and their location in the sample, it is inferred that melting of the metallic precipitates occurred before melting of the (U, Zr)O_2 mixed oxide during the VERDON-4 test. Once these precipitates were in contact with the molten $U_yZr_{1-y}O_{2\pm x}$ phase, they migrated more easily towards the periphery of the sample and coalesced as they were blocked by the cladding. It is highly consistent with the melting temperature of metallic precipitates and the $U_yZr_{1-y}O_{2\pm x}$ phase calculated by thermodynamics.

In the case of VERDON-3, despite the calculated melting temperature of the metallic precipitates (2120 °C), no clear experimental evidence of their melting could be

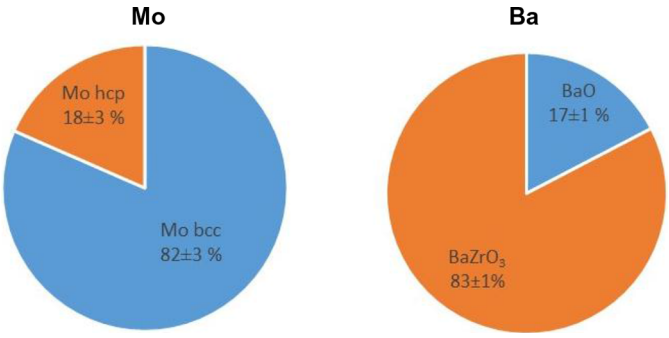

Fig. 5. Linear combination fitting results performed between −20 and +60 eV around Mo K-absorption edge and Ba L_3-absorption edge of the $T_{0(SIMF)}$ sample.

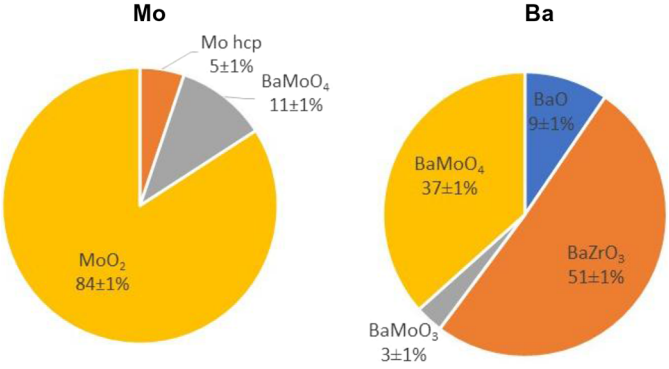

Fig. 6. Linear combination fitting results performed between −20 and +60 eV around Mo K-absorption edge and Ba L_3-absorption edge of the O1000 sample.

brought besides their rounded shape and mobility during the test. Indeed, they were found to be mainly located in the Pu agglomerates in the father rod ($T_{0(IF)}$), whereas they were homogeneously distributed in the VERDON-3 fuel sample.

Globally, a homogenization of the fuel composition has thus been observed after the VERDON-3 test compared to the as-irradiated father rod whereas the fuel heterogeneity has been conserved after the VERDON-4 test. This phenomenon can thus be attributed to the enhanced metallic precipitates mobility in oxidizing conditions at high temperature. The evolution of the fuel played also an important role on the metallic precipitates' behaviour as the presence of a $U_yZr_{1-y}O_{2\pm x}$ phase in reducing conditions involved their coalescence after melting.

3.2 Interactions between Mo and Ba under oxidizing atmosphere

Ba and Mo were initially found in two types of phases in the $T_{0(SIMF)}$ sample consistently with the literature [16]. Complementary with the SEM-EDX results, XANES enabled to quantify the amount of element involved in each phase as well as identifying its crystallographic structure.

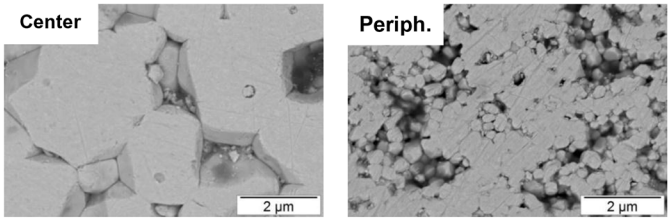

Fig. 7. SEM-BSE images showing the morphology of the grains in the centre (left) and the periphery (right) of the pellets of batch 3 ($UO_2 + 1.2\%$ $Cs_2U_xO_y$).

- Mo was found in metallic precipitates alone in a bcc structure or with Ru, Rh and Pd in a hcp structure according to the XANES results shown in Figure 5. These precipitates are also observed in PWR irradiated fuels in normal operating conditions. No MoO_2 has been detected at the initial state in the SIMFuel samples, which is consistent with the strongly reducing atmosphere of the sintering.
- Ba was found in oxide precipitates mainly whether as a simple oxide BaO (17% according to the XANES results shown in Fig. 5) or as a more complex one known as grey phase (Ba, Sr)(Zr, U, RE)O_3 (where RE stands for Rare Earth).

At 1000 °C under oxidizing conditions, Mo has partially oxidized to form MoO_2 according to the XANES analyses (Fig. 6).

In the same range of temperature, a reaction between Mo and Ba led to partial decomposition of $BaZrO_3$ into ZrO_2 and $BaMoO_4$ (Fig. 6). This reaction has been inferred to an enhanced diffusion of Mo in oxidizing conditions: Mo would first dissolved as MoO_2 in the UO_{2+x} matrix, and might have migrated from the metallic to the oxide precipitates driven by a gradient of O concentration. It would then react with the Ba contained in $BaZrO_3$.

3.3 Estimation of the oxygen potential during SPS of SIMFuel samples

After sintering, pellets of batch 3 were polished and observed by means of SEM (Fig. 7). The grain size is higher in the centre of the pellets ($2.45 \pm 0.17\,\mu m$) compared to the periphery ($0.62 \pm 0.13\,\mu m$). This phenomenon has already been observed in the study by [12]. This microstructure gradient was attributed to a higher oxidation state in the bulk of the samples compared to the surfaces due to a probable interaction between UO_{2+x} (where $x = 0.01$ in the study by [12]) and the graphite matrix according to reaction (1):

$$UO_{2+x} = xC \rightarrow UO_2 + xCO. \quad (1)$$

The XANES spectral signature of Cs in a sample of batch 3 is very close to the one of $Cs_2U_xO_y$ (Fig. 8). Thus, Cs would still be present in the sample as uranates.

Table 3. Concentration in U, Mo and Cs remaining in the samples of batch 3 after sintering at 1200 °C during 5 min, obtained through ICP-MS and ICP-AES.

Batch	U concentration (mg/g_{sample})	Cs concentration (mg/g_{sample})	% Cs remaining in the sample
UO_2 + 1.2% $Cs_2U_xO_y$	870.9 ± 17.4	2.706 ± 0.271	55 ± 6

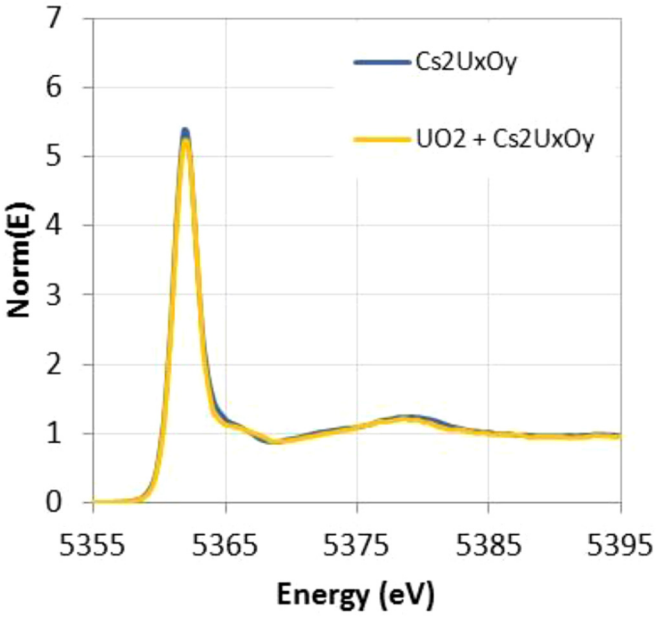

Fig. 8. Experimental HERFD-XANES spectra of $Cs_2U_xO_y$ standard and a sample of batch 3 as-sintered acquired on the FAME-UHD beamline (ESRF).

However, ICP-AES results showed that around half of the initial Cs amount had been volatilized during sintering (Tab. 3).

According to Figure 9, at 1200 °C Cs can be present as free Cs (gaseous in these conditions) or under uranate condensed forms. These phases are both consistent with the experimental observations. The release of Cs at 1200 °C results from the decomposition of uranates to form free Cs according to $Cs_2UO_4 \rightarrow UO_2 + 2\ Cs + O_2$.

Considering the experimental data, Cs and Cs_2UO_4 coexist in the samples of batch 3. As shown in Figure 9, the oxygen potential range during sintering is thus probably located around the limit between the $UO_2 + Cs_2UO_4$ and $UO_2 + Cs_{(l)}$ domains, which also corresponds to the area between the $C_{(s)}/CO_{(g)}$ equilibrium at 1 bar and the oxygen potential corresponding to $UO_{2.00}$. This domain is pointed out thanks to the grey circle on Figure 9, and extends from –550 kJ $mol_{(O2)}^{-1}$ to −475 kJ $mol_{(O2)}^{-1}$.

In order to check the validity of this hypothesis, the samples of batch 8 were characterized by SEM-EDX. Ba and Cs were often found together but no chemical contrast could be observed in BSE mode (Fig. 10). This is probably because Ba and Cs are associated to U and O, the mass of Ba or Cs uranates being quite close from the one of UO_2. Some Mo was observed alone as well as some Cs and Ba. These observations suggest that no $BaMoO_4$ remained in the sample and apparently no Cs_2MoO_4 was formed.

According to the predominance diagram established for batch 8 (Fig. 11), the decomposition of $BaMoO_4$ suggested by the SEM-EDX analyses would occur at 1200 °C below −325 kJ $mol_{(O2)}^{-1}$. Concerning Cs, it is calculated to be present either as free Cs or Cs_2MoO_4 at thermodynamic equilibrium at 1200 °C. Mo is calculated to be present either as Cs_2MoO_4 or metallic Mo below −370 kJ $mol_{(O2)}^{-1}$. The only oxygen potential range allowing to explain the absence of $BaMoO_4$ and Cs_2MoO_4 in the samples, is the one proposed in Figure 9 (–550 kJ $mol_{(O2)}^{-1}$ to −475 kJ $mol_{(O2)}^{-1}$).

4 Conclusion

Two types of samples have been studied in detail in this study: irradiated MOX fuels and SIMFuels produced through sintering at high temperature (1650 °C, 2 h, H_2 atmosphere). The samples were submitted to thermal treatments in conditions representative of a PWR severe accident. This approach made it possible to cover a temperature range from 400 °C up to 2530 °C and oxygen potentials from −470 kJ $mol_{(O2)}^{-1}$ to –100 kJ $mol_{(O2)}^{-1}$. The samples were characterized before and after each test using complementary techniques like OM, SEM, EPMA and SIMS in the case of irradiated fuels. XANES measurements using synchrotron radiation facilities were also performed on SIMFuels and produced valuable results on FP speciation (oxidation state, crystallographic structures, etc.).

The main phenomena assessed in the scope of this work were:

- Effect of fuel-cladding interactions on the fuel's melting temperature. It seems that the role of the oxygen potential in this phenomenon is to enhance the diffusion of species in oxidizing conditions. The $U_{1-x}Zr_xO_{2\pm x}$ composition for which the melting temperature is minimal is thus reached earlier than in the case of a reducing atmosphere.
- Interactions between Mo and the oxide phase containing Ba, which has been described in the present paper. These interactions were shown to occur at temperatures as low as 1000 °C under oxidizing conditions. The formation of MoO_2 and its reaction with $BaZrO_3$ results in the breakdown of this phase into $BaMoO_4$ and ZrO_2.
- The composition and behaviour of metallic phases in severe accident conditions. Mo depletion of the Mo-Ru-Rh-Pd-Tc inclusions was observed to take place around

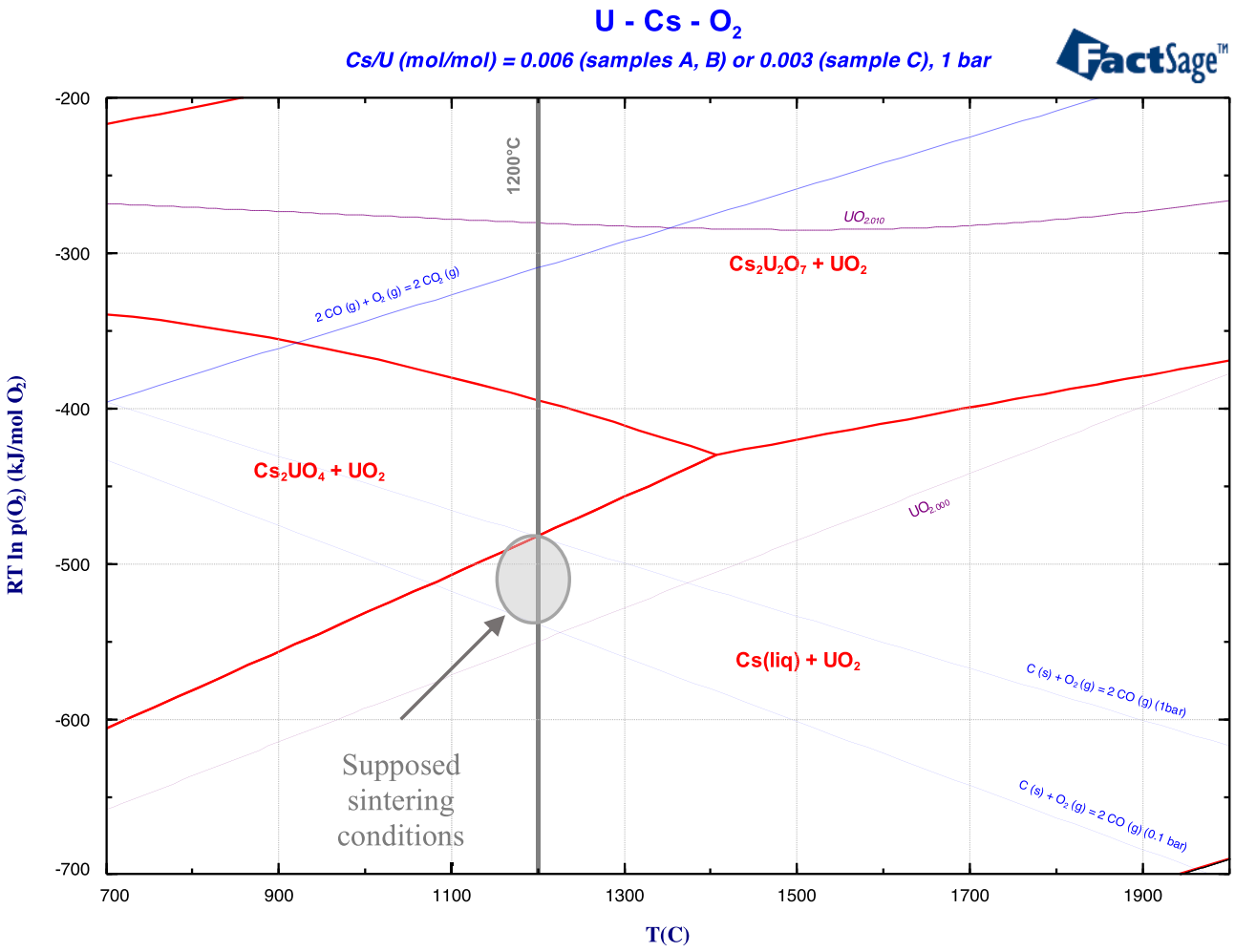

Fig. 9. Predominance diagram for the Cs-U-O_2 system (Batch 3), considering the quantities of elements remaining in the system after sintering (obtained using the SGPS database of FactSage [3,4]).

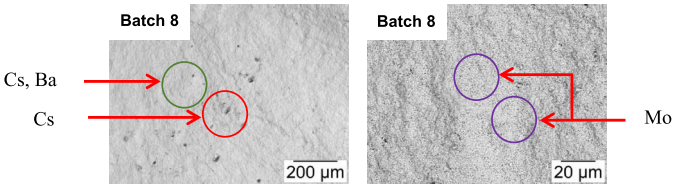

Fig. 10. SEM-BSE images of fractured surfaces of a sample of batch 8 ($UO_2 + 4.0\%$ $Cs_2U_xO_y + 4.0\%$ $BaMoO_4$) of the SPS-2 series.

1000 °C in oxidizing conditions because of the oxidation of Mo into MoO_2. In reducing conditions, no major composition changes were observed.

More generally, the principal limitation of this approach lies in the behaviour of volatile FP such as Cs. These FP are released relatively quickly during a severe accident and are totally released from the fuel above 2300 °C. Thus, the characterizations performed on irradiated fuels before and after a full accident sequence provided very little information on volatile FP speciation. Much in the same way, volatile FP are volatilised during the sintering stage of the SIMFuel fabrication process produced at high temperature, thus preventing their study at intermediate temperature levels.

Thus, low-temperature sintering was investigated for the production of SIMFuel samples containing Cs, Mo and Ba. Cs proved to remain in the samples obtained through SPS (1200 °C, 5 min, Ar atmosphere). Moreover, the chemical state of these three FP in the pellets is representative of that in the centre of PWR fuels under normal operating conditions. Despite these promising results, large Cs and Mo releases occurred during sintering and the additives in the pellets were not distributed homogeneously. These issues brought us to consider further development of this production route.

Throughout this study and beyond the results presented in this paper, thermodynamic calculations were performed to assess the FP and fuel chemical state in the different conditions and materials in question. These calculations proved to be a necessary tool to interpret the experimental data obtained. The key contributions of

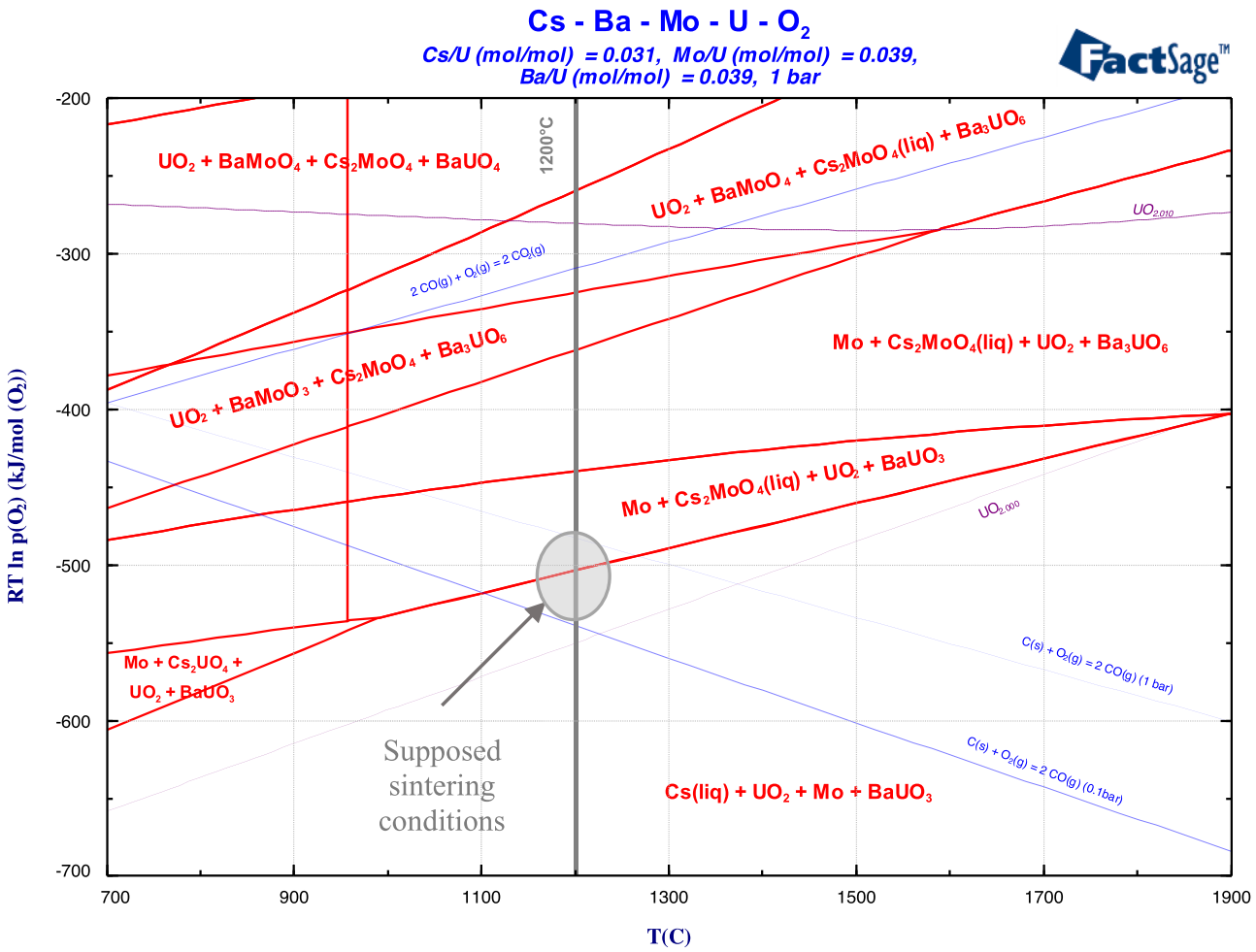

Fig. 11. Predominance diagram for the U-Cs-Ba-Mo-O_2 system (Batch 8), considering the quantities of elements added before sintering, obtained using the SGPS database of FactSage [3,4].

thermodynamics in this work are:

- Interpretation of the VERDON-3 and 4 scenarios in term of FP speciation and fuel behaviour. The calculations coupled with the experimental data led to the proposal of a mechanism for FP speciation adapted to each test. However, the assumptions used in these calculations (considering the whole irradiated fuel-FP-cladding systems) showed some limitations.
- Choice of the experimental conditions in which thermal treatments were led on SIMFuels so as to observe a chemical evolution of Ba and Mo in the samples.
- Determination of the oxygen potential range within which the SIMFuels were manufactured in the SPS furnace, as detailed in the present paper. The sintering range was defined between $-550\,\mathrm{kJ\,mol_{(O2)}}^{-1}$ to $-475\,\mathrm{kJ\,mol_{(O2)}}^{-1}$ at 1200 °C.

Today, there is no longer any doubt concerning the existing link between fission products' chemical behaviour in the fuel and their release. Although their behaviour in the fuel during a severe accident is mainly governed by thermochemistry, this work demonstrated that it cannot be separated from the kinetics aspect. Indeed, chemical reactions between the different elements are strongly impacted by the ability of the different fission products to diffuse through the fuel pellets, which is insufficiently taken into account in the release models.

The authors are grateful to EDF who financed the analyses of irradiated fuel samples. We are highly indebted to the CEA / SA3E / LCPC and LARC staffs who performed respectively the experimental characterizations on the irradiated fuel samples and the ICP-AES / MS analyses. We would also like to thank the staffs of the MARS, FAME and FAME-UHD beamlines for their key contribution in the study of FP speciation in SIMFuels thanks to XANES. We are also grateful to the teams of the CEA / SCCME / LM2T and CEA / SESC / L2EC for their decisive participation to the thermodynamic calculations respectively with ThermoCalc and Factsage. Finally, we are truly thankful to the staff of the Joint Research Centre of Karlsruhe, directorate G, as well as to the GENTLE program for having accepted and financed our experiments on their SPS device.

Author contribution statement

The study presented in this article has been carried out in the frame of Claire Le Gall's Ph.D. thesis supervised by Fabienne Audubert, Jacques Léchelle and Yves Pontillon from the CEA and Jean-Louis Hazemann from the CNRS / ESRF. Claire Le Gall has written this article. Fabienne Audubert, Jacques Léchelle, Yves Pontillon and Jean-Louis Hazemann have contributed to this work by providing support through proofreading and expert viewpoints on the different aspects of this article.

References

1. J.-O. Andersson et al., Calphad **26**, 273 (2002)
2. TAF-ID, working version of january 2018, https://www.oecd-nea.org/science/taf-id/
3. C.W. Bale et al., Calphad **26**, 189 (2002)
4. C.W. Bale et al., Calphad **33**, 295 (2009)
5. A. Gallais-During et al., in *21st International Conference Nuclear Energy for New Europe*, *2012*
6. C. Le Gall, Ph.D. thesis, Université Grenoble Alpes and CEA Cadarache, 2018
7. Cesar 5.1, developed by DEN/DER/SPRC, CEA Cadarache
8. P.G. Lucuta et al., J. Nucl. Mater. **178**, 48 (1991)
9. Z. Hiezl, Ph.D. thesis, Imperial College London, 2015
10. Y. Pontillon et al., European Working Group «Hot Laboratories and Remote handling», 2005
11. Y. Joly, Phys. Rev. B **63**, 125120 (2001)
12. V. Tyrpekl et al., Sci. Rep. **7**, 46625 (2017)
13. D.W. Osborne et al., J. Chem. Thermodyn. **8**, 361 (1976)
14. A. Labet et al., in *European Winter Conference on Plasma Spectrometry*, *2019*
15. E. Geiger et al., J. Nucl. Mater. **495**, 49 (2017)
16. H. Kleykamp, J. Nucl. Mater. **131**, 221 (1985)

Cite this article as: Claire Le Gall, Fabienne Audubert, Jacques Léchelle, Yves Pontillon, Jean-Louis Hazemann, Contribution to the study of fission products release from nuclear fuels in severe accident conditions: effect of the pO_2 on Cs, Mo and Ba speciation, EPJ Nuclear Sci. Technol. **6**, 2 (2020)